ORIGINAL RESEARCH ARTICLE

Physicochemical and Biological Characterization of RTXM83, a New Rituximab Biosimilar

María L. Cerutti[1,3] · Analía Pesce[1] · Cédric Bès[2] · Mauricio Seigelchifer[1]

Abstract

Background RTXM83 is a rituximab biosimilar with proven clinical safety and efficacy. It is the first rituximab biosimilar developed and approved in South America and is currently marketed in several Latin American, Middle Eastern and African countries.

Objective The aim of this study was to present the physicochemical and biological characterization studies utilized to demonstrate the similarity between RTXM83 and its reference product.

Methods Primary and higher order protein structures were analysed using peptide mapping with liquid chromatography–electrospray ionization–tandem mass spectrometry (LC–ESI–MS/MS), fluorescence spectroscopy and circular dichroism, and micro-differential scanning calorimetry, among other techniques. Charge variants were determined by cation-exchange chromatography (CEX) and capillary isoelectric focusing (cIEF). Glycosylation and glycoforms distribution were analysed using MS, normal phase high-performance liquid chromatography (NP-HPLC) and high-performance anion-exchange chromatography with pulsed amperometric detection (HPAE-PAD). Size variants were evaluated by size-exclusion chromatography (SEC), sedimentation velocity analytical ultracentrifugation (SV-AUC), dynamic light scattering (DLS), and capillary electrophoresis-sodium dodecyl sulfate (CE-SDS). Biological characterization included binding assays for complement C1q, CD20, and several Fc receptors (FcRs), as well as potency determination for in vitro apoptosis induction, complement-dependent cytotoxicity (CDC), and antibody-dependent cell-mediated cytotoxicity (ADCC).

Results RTXM83 and the reference product showed identical primary sequences and disulfide bridge patterns, and similarity at higher order protein structures, post-translational modification profiles (amino acid modifications, charge variants, and glycosylation) and levels of purity and process-related impurities. Functional studies demonstrated that RTXM83 is similar to the reference product regarding the three known mechanisms of action of rituximab: CDC, ADCC, and apoptosis induction. Binding affinities to CD20, complement component C1q, and different FcRs were also equivalent.

Conclusion RTXM83 is similar to its reference product in all critical quality attributes.

1 Introduction

Rituximab is a chimeric human-murine IgG1 monoclonal antibody (mAb) directed against the human transmembrane protein CD20, a surface marker highly expressed on most malignant B

✉ Mauricio Seigelchifer
mauricio.seigelchifer@mabxience.com

1 mAbxience, Carlos Villate 5148, Munro, B1605AXL Buenos Aires, Argentina

2 mAbxience, Madrid, Spain

3 Present Address: Fundación Instituto Leloir-IIBBA-CONICET, Buenos Aires, Argentina

Key Points

RTXM83 and the reference product show identical primary sequences and disulfide bridge patterns, and high similarity in all tested physicochemical properties: higher order structure, post-translational modifications, high molecular weight aggregates, and purity.

RTXM83 is similar to the reference product regarding all three described mechanisms of action of rituximab: antibody-dependent cell-mediated cytotoxicity, complement-dependent cytotoxicity, and apoptosis induction.

RTXM83 is the first rituximab biosimilar developed and approved in South America, and is marketed in several low-income countries.

cells [1]. In the late '90s, the demonstrated high efficacy of rituximab to deplete CD20+ peripheral blood B cells in patients with recurrent B-cell lymphoma [2, 3] led to its approval as the first therapeutic mAb for cancer treatment by the US Food and Drug Administration (FDA) and European Medicines Agency (EMA) as Rituxan®/MabThera®. Since then, rituximab has become a worldwide standard component of care for several CD20+ B-cell malignancies [4] and has acquired approval for the treatment of various autoimmune disorders such as rheumatoid arthritis, Wegener's granulomatosis and microscopic polyangiitis [5, 6].

Biosimilars are biologic drugs designed to be similar to a licensed or approved biologic product (''the reference medicinal product'', RMP) for which patents have expired. To be similar in efficacy, safety, and immunogenicity, biosimilar medicines should be developed to fulfil the requisites established in the guidelines of international regulatory agencies such as the EMA [7], World Health Organization (WHO) [8], FDA [9] and different Latin American countries [10–15]. Biosimilarity should then be demonstrated through a comparability exercise in which the RMP critical quality attributes (CQAs) are compared against those of the proposed biosimilar product.

Unlike biologics produced in microbial hosts, the manufacture of complex glycosylated biosimilar agents such as mAbs, epoetin, and gonadotropins requires them to be produced in mammalian cell culture systems, which are highly sensitive to bioprocess conditions [16, 17]. There are currently two different rituximab biosimilar products that have been approved in Europe: one from Celltrion and the other from Sandoz. In the United States, only the Celltrion's rituximab biosimilar got approval. RTXM83 is a rituximab biosimilar developed under the rigorous guidelines of international regulatory agencies. Previous functional studies have demonstrated that it is similar to the MabThera®/Rituxan® reference product regarding its binding capacity to CD20+ human cells and antibody-dependent cell-mediated cytotoxicity (ADCC) potency [18], even in relation to the reported differential sensitivity of rituximab to the phenylalanine/valine (F/V) polymorphism at position 158 in the FcγRIIIa receptor [19–21]. More recently, its clinical efficacy, safety, and tolerability [22] have led to its approval as the first rituximab biosimilar in South America and its marketing in several Latin American, Middle Eastern and African countries. In this work, we present an extended characterization of RTXM83 by describing part of the "totality of evidence" built to demonstrate its physicochemical and biological similarities to the reference product.

2 Materials and Methods

2.1 Materials

More than 20 batches of MabThera® and Rituxan® were sourced from different regions (i.e. the EU, the USA, and Argentina) and used to establish the CQA similarity ranges and perform comparability studies as the rituximab reference product material. The RTXM83 biosimilar was produced in-house as previously described [18].

2.2 Peptide Mapping Analysis

Rituximab samples (100 μg) were denatured and reduced in the presence of guanidinium hydrochloride and dithiothreitol (DTT). After treatment with iodoacetamide, the samples were dialysed against buffer containing 0.8 M urea and were digested with trypsin or Endo Lys-C proteases. The resulting peptides were separated by reversed phase high-performance liquid chromatography (RP-HPLC) using an Acclaim PepMap RSLC C18 column (2 μm; 0.3 × 150 mm; Thermo Scientific, Germany). For disulfide bond analysis, rituximab samples (150 μg) were incubated with N-ethylmaleimide and denatured with 6 M guanidine hydrochloride. The samples were then dialysed against phosphate buffer containing 0.8 M urea and were digested for 3 h with 2% (weight per weight [w/w]) Endo Lys-C followed by an additional 14-h incubation with 2.5% (w/w) trypsin. The resulting peptides were separated using an Aeris Peptide XB-C18 column (3.6 μm; 4.6 × 250 mm; Phenomenex, Germany). The primary sequence determination, amino acid modifications, and N- and C-terminal integrity spectra were recorded in the mass range of 200–2500 Da in the positive ion mode. Mapping spectra for disulfide determinations were recorded in the mass-to-charge ratio (m/z) range of 50–2000 in the positive ion mode. The LC-ESI-MS/MS data were deconvoluted using DataAnalysis v4.2 software (Bruker Daltonics, Bremen, Germany). In all chromatographic analyses, the absorbance was monitored at 214 nm using an Ultimate 3000RSLC HPLC nano system (Thermo Scientific) coupled to a maXis 3G ESI-QTOF mass spectrometer (Bruker Daltonics, Bremen, Germany).

2.3 Molecular Weight Determinations

The molecular weights of intact or reduced (deglycosylated or non-deglycosylated) RTXM83 and RMP samples were determined by liquid chromatography-electrospray ionization-mass spectrometry (LC–ESI–MS). For de-N-glycosylation treatment, antibody samples (500 μg) were reduced with 50 mM of 2-mercaptoethanol and were subjected to PNGase F treatment (Prozyme, CA, USA) overnight at 37 °C. The digested samples were separated in a reversed-phase ProSwift RP-4H LC column (1 × 50 mm; Thermo Scientific), and the signal was monitored at 214 and 280 nm. Spectra were recorded in the positive ion mode in the mass range between 1200 and 5200 m/z and were deconvoluted using the maximum entropy algorithm of DataAnalysis v4.2 software (Bruker Daltonics).

2.4 Fluorescence Measurements

Tryptophan fluorescence spectra were performed using a FP-6200 Jasco spectrofluorometer with excitation at 280 nm and an emission spectral range between 250 and 470 nm. The scan speed was 60 nm/min, and data pitch was 1 nm. The samples were measured in phosphate buffer pH 7.0 at a 0.2-mg/ml protein concentration in a 10-mm cuvette path length.

2.5 Circular Dichroism Experiments

Far-UV circular dichroism (CD) measurements were carried out in a Jasco J-715 spectropolarimeter using a cell with a 0.1-cm path length. The protein samples were diluted to 0.2 mg/ml in sodium phosphate buffer pH 7.0. The acquisition parameters were as follows: 0.1-nm data pitch; 20-nm/min scanning rate; 2-nm bandwidth; and three accumulations at 25 °C. Data processing and manipulation were carried out using proprietary Jasco software, and circular dichroism analysis using neural networks (CDNN) was used for secondary structure element calculation.

2.6 Fluorescence and Static Light Scattering Thermal Stability Studies

Experiments were performed in an Optim® 1000 system (Avacta Analytical Ltd., UK) using a thermal step-ramp type experiment. Fluorescence spectra were recorded by setting the excitation wavelength at 266 nm and registering the emission from 300 to 400 nm. To detect small and large aggregates, static light scattering (SLS) was recorded at 266 nm and 473 nm, respectively. The thermal ramp was increased from 25 to 95 °C in 1-°C steps. The data were recorded and analysed using Optim® 1000 software.

2.7 Micro-Differential Scanning Calorimetry

Calorimetric analysis of the samples was performed using the Micro-Cal VP-Capillary DSC system (GE Healthcare). Samples were diluted to 2.0 mg/ml and cooled to 5 °C in the autosampler system before analysis. The instrument scanned each sample over a temperature range of 10 to 100 °C at a rate of 60 K/h. The temperature of unfolding (T_m) values were determined from the peak maxima of the deconvoluted unfolding transitions after baseline subtraction. Data analysis was done using Origin 7 DSC software.

2.8 Cation-Exchange Chromatography

Charge variant analysis was performed using a Mab-Pac SCX-10 column (10 µm; 4 mm × 250 mm; ThermoFisherScientific) connected to a Dionex GmBH, BioLC HPLC/UV system. Samples (50 µg) were injected, and UV detection was performed at 214 nm.

2.9 Glycan Analysis

For *N*-glycan analysis, antibody samples (500 µg) were treated with PNGase F as described in Sect. 2.3. *N*-glycans were labelled with 2-aminobenzamide (2-AB) and were separated by normal phase high-performance liquid chromatography (NP-HPLC) on an HPLC system with fluorescence detection (Dionex, CA, USA). Monosaccharide components were liberated from *N*-glycans by acid hydrolysis. Quantitative high-performance anion-exchange chromatography with pulsed amperometric detection (HPAE-PAD) analysis was performed using a CarboPac PA20 column (6.5 µm; 3 × 150 mm; Dionex). Quantification was calculated against a mixture of monosaccharide reference standards. For sialic acid quantification, antibody samples were subjected to mild acid hydrolysis with 5 mM sulphuric acid. Released sialic acid residues were quantitated via HPAE-PAD. Chromatography was performed using an ICS-5000+ ion chromatography system (ThermoFisherScientific Inc., MA, USA) using a high-resolution CarboPac PA200 column (5.5 µm; 3 × 250 mm; Dionex, Thermo Scientific, Germany). The amounts of *N*-acetylneuraminic (NANA) and *N*-glycolylneuraminic (NGNA) sialic acids were calculated from calibration curves with standards.

2.10 Size-Exclusion Chromatography

Size-exclusion chromatography (SEC) was performed by applying 5 µg of each rituximab sample into a TSK-gel SuperSW3000 column (4 µm; 4.6 × 300 mm; Tosoh Bioscience GmBH, Germany) connected to HPLC Dionex equipment (Sunnyvale, CA, USA). UV detection was carried out at 214 nm. The data were acquired and processed using Chromeleon Chromatography Management System v6.8.

2.11 Sedimentation Velocity Analytical Ultracentrifugation Determinations

Sedimentation velocity analytical ultracentrifugation (SV-AUC) experiments were performed on an Optima-XLA analytical ultracentrifuge using an An-50 Ti rotor (all Beckman Coulter, Nyon, Switzerland). The samples were diluted to 0.75 mg/ml in phosphate-buffered saline immediately prior to measurement. UV detection was set at 280 nm, and the rotor speed was set for 45,000 rpm. The data were analysed using SEDFIT software (v11.91), and the distribution of sedimentation coefficients (S_m) was determined with the c(s) model.

2.12 Fab-Related Functions

Antibody binding to membrane-bound CD20 was determined by a cell-based enzyme-linked immunosorbent assay (ELISA) with electrochemiluminescence detection (Meso Scale Discovery, MSD, USA). Briefly, Jeko-1 cells (3×10^5 cells/ml) were coated on high-binding plates and incubated with serial dilutions of rituximab samples (40 µg/ml of stock solution). Detection was performed using a strep-Sulfotag conjugated antibody, and the electrochemical luminescent signal was read on a SECTOR Imager 2400 reader (MSD, USA). Apoptosis was determined using the FITC Annexin V Apoptosis detection kit (Becton Dickinson, Germany). Briefly, human Ramos cells (2×10^6 cells/ml) were incubated with serial dilutions of rituximab (19.4 µg/ml of stock solution) for 26 ± 2 h and were stained with Annexin V-FITC and propidium iodide according to the instructions of the supplier. The samples were measured on a FACSCalibur flow cytometer, and data were acquired using Cell Quest software (all Becton Dickinson, Germany).

2.13 Fc-Related Biological Functions

C1q binding was measured by ELISA according to Idusogie et al. [23]. Briefly, assay plates were coated with serial antibody dilutions (30 µg/ml of stock solution) and were blocked with 0.1% gelatine. Subsequently, the plates were incubated with human C1q followed by an anti-human C1q-conjugated polyclonal antibody. For complement-dependent cytotoxicity (CDC) determinations, Ramos cells (5×10^4 cells/well) were pre-incubated with serial antibody dilutions (1.2 µg/ml of stock solution). CDC activity started upon the addition of baby rabbit complement (Bio-Rad AbD Serotec, Germany), and the effect was analysed by luminescence readout using the CellTiter-Glo® Luminescent Cell Viability Assay (Promega, Germany). Samples were measured using an Infinite M200 Luminescence microplate reader (Tecan, Swiss). ADCC activity was measured using the ADCC Reporter Bioassay Core Kit (Promega, Germany). Target Ramos cells (2.5×10^4 cell per well) were incubated with serial dilutions of rituximab samples (6.0 µg/ml of stock solution) for 30 min. Subsequently, target cells were mixed with the genetically engineered Jurkat T NFAT-RE-luc effector cells at an effector cell:target cell ratio of 6:1. Luciferase activity was quantified using the Bio-Glo™ Luciferase Assay System (Promega, Germany) after 6 h of incubation.

The affinity to recombinant human Fcγ receptors FcγRI, FcγRIIa, FcγRIIb, and FcγRIIIa and the neonatal Fc receptor (FcRn) was determined by surface plasmon resonance (SPR) using Biacore T200 and 4000 instruments (GE Healthcare, Freiburg, Germany). The different Fc receptors (FcRs) were covalently immobilized on carboxymethyl-dextran-coated CM5 sensor chips using standard amine coupling chemistry.

Equilibrium dissociation constant (K_D) values were determined using Biacore Evaluation software. Formal qualification was performed on the relative binding responses.

2.14 Statistical Analysis

All relative biological activity and binding potency determinations were carried out against an RTXM83 in-house reference standard. Statistical analysis was calculated using PLA 2.0 software (Stegmann Systems GmbH, Germany) considering a 95% confidence interval (CI) for linearity, parallelism and regression significance and potency estimation.

3 Results

3.1 Primary Structure, Disulfide Linkages and Amino Acid Modifications

Rituximab is an IgG_1Vk antibody of 1328 amino acid (aa) residues that consists of two light chains (LCs) and two heavy chains (HCs) of 231 and 451 aa, respectively [24]. The HCs and LCs are connected via 12 intrachain and four interchain disulfide linkages, and HCs have one conserved N-glycosylation site at the CH2 asparagine 301 (Asn301). Similar to many other recombinant mAbs, rituximab presents two major modifications due to bioprocess conditions: first, the cyclization of the HC and LC N-terminal glutamines to pyroglutamic acid (pyroGlu), leading to a mass decrease of 17 Da due to ammonia loss; second, the cleavage of the C-terminal lysine, which decreases the mass of the mAb by 128 Da [25].

We initiated our physicochemical comparability exercise by assessing the degree of amino acid sequence identity existent between RTXM83 and the RMP. LC-ESI-MS/MS peptide mapping experiments showed indistinguishable chromatograms for RTXM83 and the reference product, with similar peak intensities and retention times. No new peaks in the RTXM83 chromatograms were observed (Fig. 1). Sequence coverage was 100%.

Detailed N- and C-terminal integrity mass analysis showed that the LC and HC N-terminal glutamines of both rituximab products were almost completely modified as pyroGlu (98–99% for the LC and 100% for the HC). Additionally, the C-terminal end of the HC was detected as the peptide was modified by lysine cleavage for all samples to a similar extent (95–99%). The location of the N-glycosylation site at Asn301 in RTXM83 was also confirmed.

The position and integrity of the disulfide bonds were then assessed by non-reduced peptide mapping analyses. The eight disulfide-linked peptides expected in rituximab (Supplementary [Suppl.] Fig. 1A, see the electronic supplementary material) were identified and mapped in all

RTXM83 batches tested. The chromatograms of the biosimilar and reference product were indistinguishable (Suppl. Fig. 1B). Taken together, these data support the claim that RTXM83 and the RMP have identical amino acid sequences and disulfide linkage patterns, and present similar abundances of chemical amino acid modifications.

The molecular weight masses of intact RTXM83 and RMP IgGs were subsequently identified and compared by LC-ESI-MS. Untreated samples showed mass signals corresponding to the intact mAb with different combinations of Fc-glycosylation (146,846–147,852 Da; Fig. 2). The observed values matched the theoretical mass of the rituximab molecule bearing full pyroglutamate converted LC and HC N-terminal extremities and complete lysine cleavage of the HC C-terminus. The resolved and detected major glycoform structures were G0F/G0F, G0F/G1F, G1F/G1F or G0F/G2F, and G1F/G2F. The amount of G0F structures was slightly higher in the biosimilar. Lower levels of glycan species such as Man5, G0 and G0F-GN were detected (Fig. 2 and Suppl. Fig. 2A). Analysis of the reduced and de-*N*-glycosylated HC and LC samples showed indistinguishable patterns between products (Suppl. Fig. 2; panels B and C). The HCs mass signals of both products were detected between 49,069.4 and 49,069.8 Da, which are 145 Da smaller than the theoretical HC mass due to the mentioned N- and C-terminal modifications. Traces of uncleaved C-terminal lysine residues were observed for some RTXM83 samples. The LC mass signals corresponded with the theoretical mass of an LC with N-terminal pyroGlu modification (23,039.4 Da).

3.2 Higher Order Structure

The conformation and thermal stability of RTXM83 compared with that of the reference product were subsequently evaluated by an array of biophysical techniques.

Intrinsic fluorescence experiments revealed that RTXM83 presents features of properly folded proteins, with a maximum fluorescence intensity at 340 nm. Biosimilar overall spectra were perfectly superimposable to those of the reference product, denoting a high degree of folding similarity between products (Fig. 3a). Far-UV CD measurements indicated that RTXM83 and RMP have identical structural topologies. As expected, the CD spectra showed characteristics of β-sheet-rich proteins, exhibiting broad minima from 216 to 219 nm, followed by maxima at ~ 202 nm (Fig. 3b). Both products have a comparable composition in secondary structure: 7–8% α-helix; 40–42% antiparallel β-sheet, ca. 6% parallel β-sheet, ca. 17% β-turn, and ca. 35% random
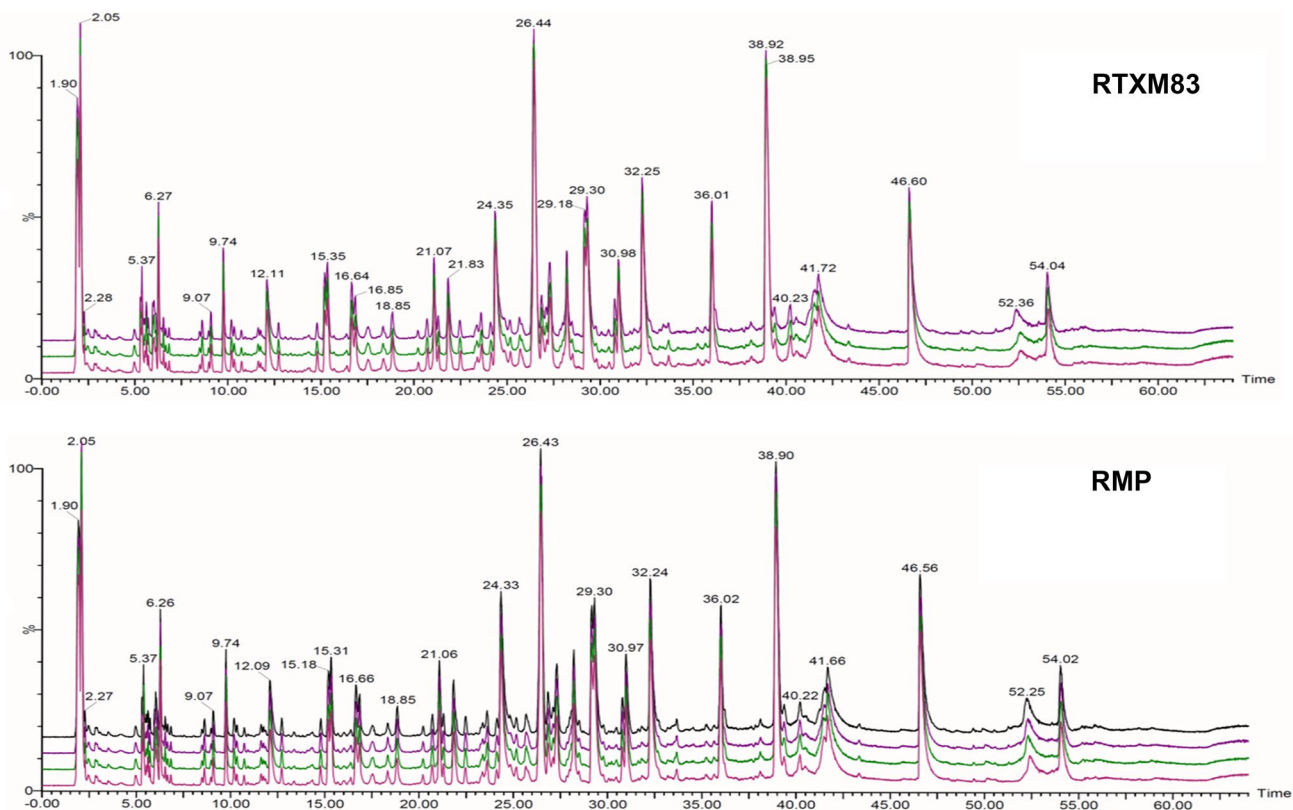

Fig. 1 Primary structure of RTXM83 and RMP. Tryptic peptide map chromatograms under non-reducing conditions. Four lots of RMP and three lots of RTXM83 are displayed. *RMP* reference medicinal product
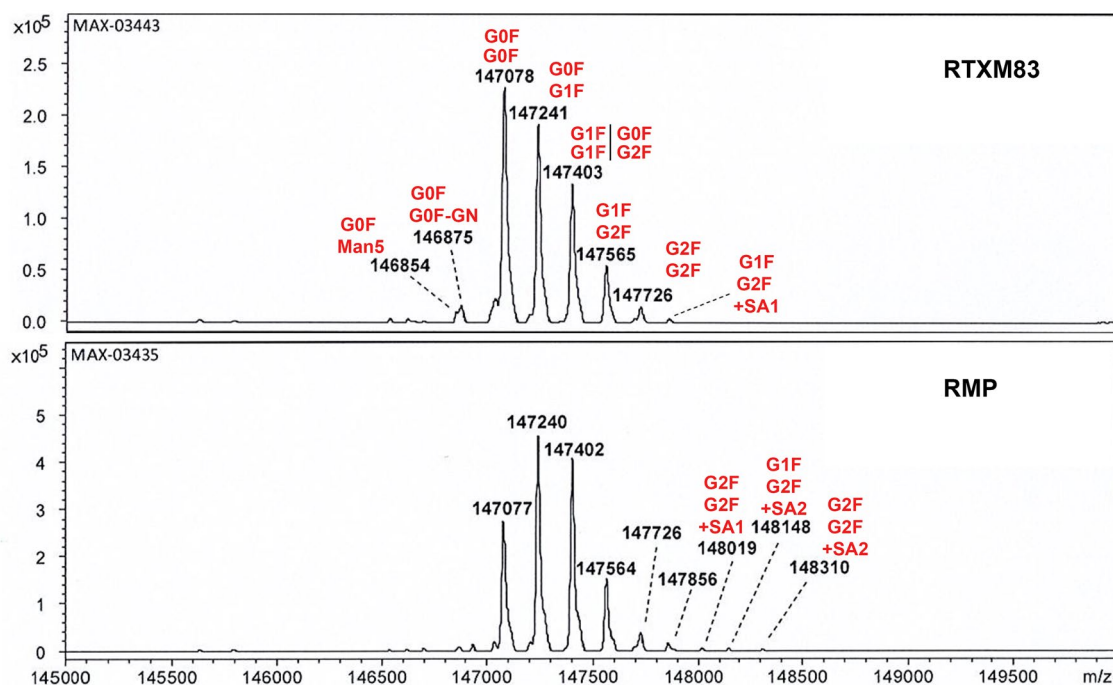
Fig. 2 Intact mass analysis. Deconvoluted mass spectra of the LC–ESI–MS analysis of native samples of RTXM83 and the reference product. Mass signals correspond to the native mAb with different combinations of Fc-glycosylation. Mass range: 145,000–150,000 Da. Glycan structures: G0F, diantennary w/o 2 β-Gal with α1,6-Fuc; G0F-GN, diantennary w/o 2 β-Gal w/o 1 GlcNAc with α1,6-Fuc; G1F, diantennary w/o 1 β-Gal with α1,6-Fuc; G2F, diantennary with α1,6-Fuc; Man5, $Man_5GlcNAc_2$; SA1, monosialylated glycans; SA2, disialylated glycans. One representative run for each sample is shown as an example. *LC–ESI–MS* liquid chromatography-electrospray ionization-mass spectrometry, *mAb* monoclonal antibody, *RMP* reference medicinal product, *w/o* without

coil. Differential scanning calorimetry thermograms showed similar melting profiles for RTXM83 and RMP (Fig. 3c). As typically observed in multidomain mAb molecules, unfolding occurred in up to three individual steps (denoted T_{m1}, T_{m2} and T_{m3}) and at highly similar temperature values (Suppl. Table 1). The total heat capacity values were also very close, ranging between 1000 and 1100 kcal/mole/°C. Fluorescence spectroscopy and SLS temperature trend measurements also showed similar unfolding transitions and almost equal values of T_m and the temperature of aggregation (T_{agg}) (Suppl. Fig. 3 and Fig. 3d). Likewise, CD thermal scans showed comparable thermal stabilities between products (Suppl. Fig. 4). All spectra showed an initial increase in the CD signal at ~ 70 °C, followed by a very steep and rapid decrease, indicating cooperative unfolding. All thermostability studies showed heat-irreversible denaturation of the samples.

3.3 Charge Variants

Charge heterogeneity in monoclonal antibodies can result from multiple sources, such as N-terminal glutamine and/or glutamic acid pyroconversion and HC C-terminal lysine processing, deamination, phosphorylation, oxidation, amino acid substitution/deletion, differential glycosylation,

glycation and proteolytic degradation (reviewed in [26, 27]). Comparability studies of the charge variants present in RTXM83 and RMP were then performed by cation-exchange chromatography (CEX) and capillary isoelectric focusing (cIEF). The CEX profiles showed similarity with respect to the content and distribution of charge variants, with no appearance of new species (Fig. 4 and Suppl. Table 2). Both products presented a main isoform (~ 60%) and minor proportions of basic and acidic variants. RTXM83 presented a slightly lower content of acidic species and a slightly higher content of basic species than RMP. These results were confirmed by cIEF studies (Suppl. Table 2). Subsequent treatment with carboxypeptidase B demonstrated that the higher proportion of basic variants observed in RTXM83 is due to partial cleavage of the HC C-terminal lysines (Suppl. Fig. 5).

3.4 Glycosylation

Glycosylation is one of the most complex post-translational modifications (PTMs). It can affect protein folding, trafficking, stability and biological activity, but also plays a critical role in the serum half-life and immunogenicity [28]. Intact IgG mass analysis is a powerful method for glycoforms identification, but it is mostly used as a rapid characterization method [29]. Therefore, we proceeded to carry out a
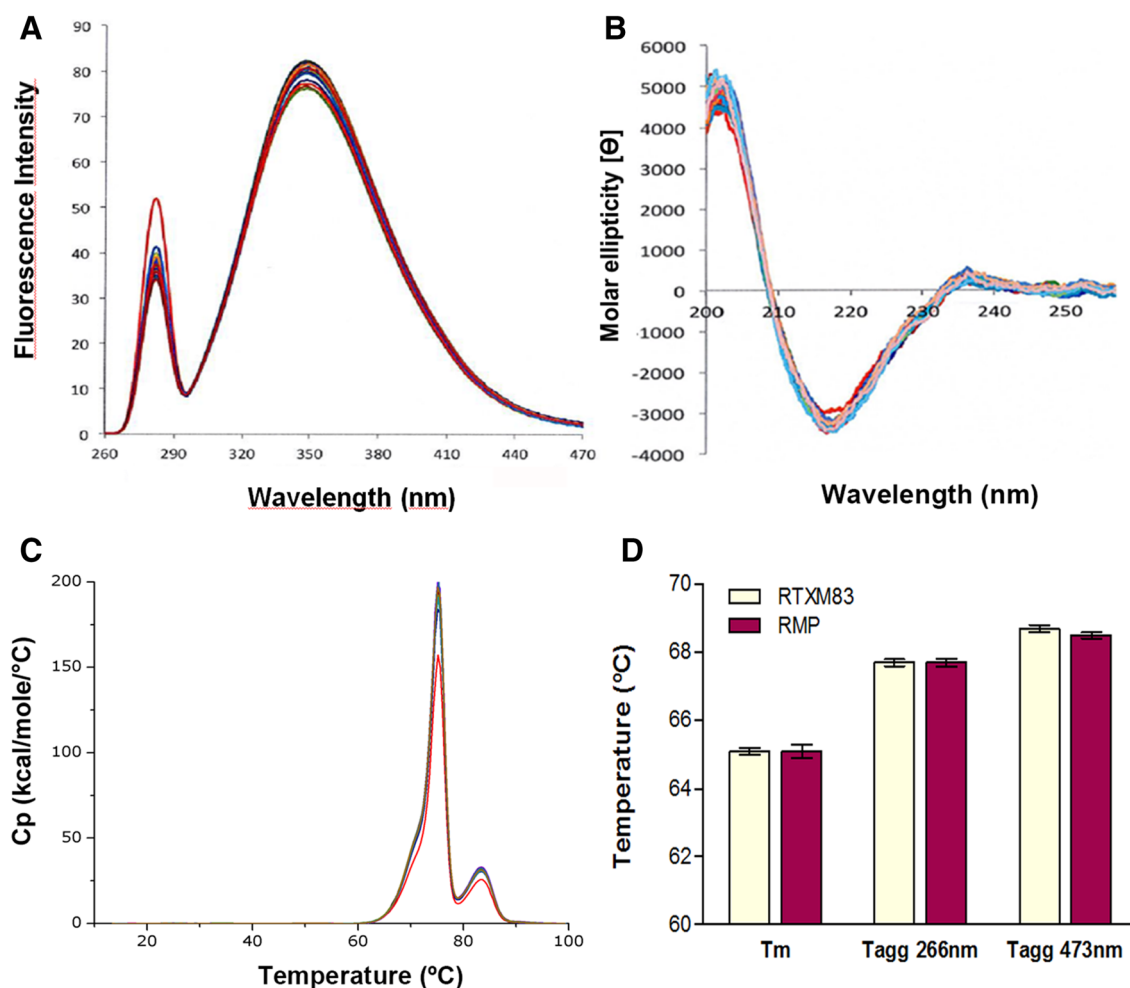
Fig. 3 Higher order structure of RTXM83 and RMP. **a** Tertiary structure and conformation by intrinsic fluorescence. **b** Secondary structure by far-UV CD spectroscopy. For **a**, **b** experiments, samples consisted of ten batches of the reference product and nine batches of RTXM83. **c** μDSC thermal unfolding curves of RTXM83 and RMP. Thermograms were obtained from analysis of the samples at ca. 2 mg/ml after baseline subtraction. **d** Thermal stability and onset aggregation by fluorescence and SLS. Bar chart showing the T_m and temperature T_{agg} values derived from the data of Supplementary Fig. 3 (see the electronic supplementary material). The data are the average plus SD of four batches of the reference product and three batches of the RTXM83 biosimilar. *μDSC* micro-differential scanning calorimetry, *C_p* Heat capacity, *CD* circular dichroism, *RMP* reference medicinal product, *SD* standard deviation, *SLS* static light scattering, *T_{agg}* temperature of aggregation, *T_m* temperature of unfolding

quantitative NP-HPLC analysis of the derivatized N-linked carbohydrates released from the mAb. In agreement with the previous intact mass studies, this analysis showed that RTXM83 and RMP have a similar overall pattern of N-glycosylation, with only minor differences in galactosylation. Total galactosylation was slightly lower for the biosimilar than for the reference product (41% vs 50.6%, respectively), which resulted in slightly higher levels of G0F and lower amounts of G1F glycoforms (47 vs 40% and 33 vs 41%, for RTXM83 and RMP, respectively; Fig. 5 and Suppl. Table 3). Total afucosylation in RTXM83 was lower than in RMP (< 2%). In agreement with these findings, HPAE-PAD analysis of monosaccharide components showed that RTXM83 had slightly lower levels of galactose (5.9 vs 7.6% for RTXM83

and RMP, respectively; Suppl. Table 3). Fucose, glucosamine and mannose residues were present at equivalent quantities in both products (Suppl. Table 3). Quantitative analysis of NGNA and NANA sialic acids demonstrated that both products have low and comparable amounts of each of these sialylated glycoforms, with only marginally higher total sialylated glycans for the reference product (Suppl. Table 3).

3.5 High Molecular Weight Aggregates and Purity

Monoclonal antibody production processes in cell cultures may originate product-related impurities such as mAb dimers or higher order aggregations, incomplete formation of the IgG molecule, and/or high levels of glycan
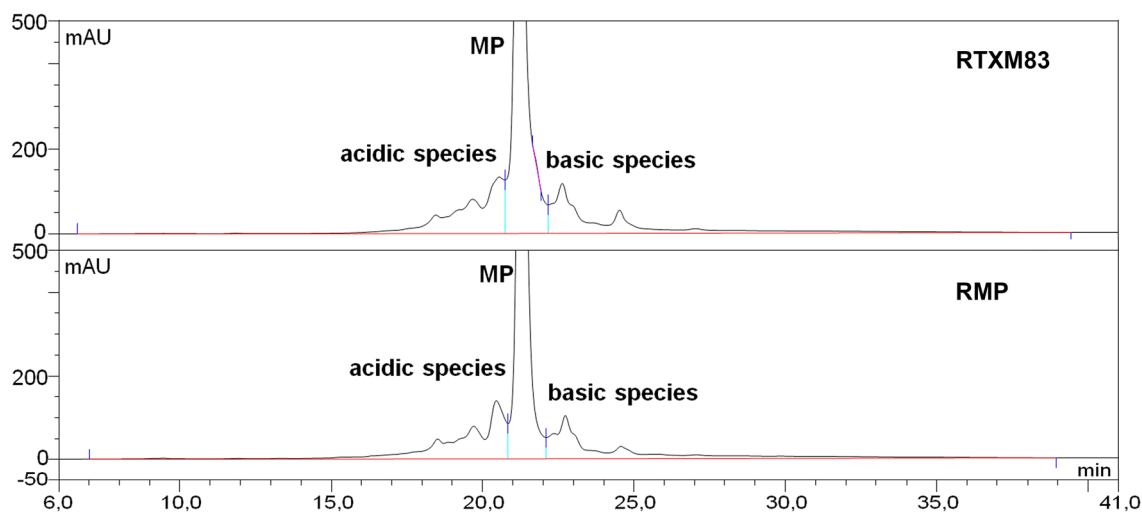
Fig. 4 Charge profiles of the RTXM83 biosimilar and RMP by CEX. Representative HPLC chromatograms of one batch from RTXM83 and one batch from the reference product (expanded scale). Integration is shown in red. The profiles of one batch from RTXM83 and one batch from the reference product are shown as examples. *CEX* cation-exchange chromatography, *HPLC* high-performance liquid chromatography, *MP* main peak, *RMP* reference medicinal product

heterogeneity [30]. Thus, the presence of aggregates in the RTXM83 samples was firstly analysed by SEC. SEC experiments showed no differences in the elution profiles of RTXM83 and RMP. Both products presented > 99% of monomeric IgG species and only 0.4–0.5% of dimers and high molecular weight (HMW) aggregates (Table 1, Suppl. Fig. 6). Considering that SEC may not always detect loosely associated or very large aggregates [31–34], SV-AUC was used as an orthogonal method to measure aggregation and fragmentation levels. In accordance with the expectation to detect mainly mAb monomers, SV-AUC studies determined one main species in the S_m range of 6.5–6.6, corresponding to a molecular weight of approximately 150 kDa in all analysed samples (Table 1 and Suppl. Fig. 7). A second marginal peak representing the dimer was detected in the S_m 9.0–9.6 S range. Additional fractions of compounds due to HMW aggregates had a low intensity (~ 1%). No low mass compounds were found in any of the tested samples. The presence of subvisible particles was additionally studied by dynamic light scattering (DLS). Similar Z-average size values were measured for both rituximab products (12.11 ± 0.08 nm and 12.05 ± 0.08 nm for RMP and RTXM83, respectively). No aggregates could be observed in any of the measured samples (Suppl. Fig. 8).

Side-by-side comparison of the reducing and non-reducing capillary electrophoresis-sodium dodecyl sulfate (CE-SDS) electrophoretic profiles revealed a similar pattern of purity and size heterogeneity among RTXM83 and the reference product (Suppl. Fig. 9 and Suppl. Table 4). Non-reducing CE-SDS experiments showed that the main

peak corresponds to whole IgG, and other species found were a single LC and a combination of two HCs and one LC (HHL). Reducing conditions showed that the content of the de-N-glycosylated heavy chain (DHC) and LC/HC ratio were similar. Additionally, comparative accelerated stability studies conducted on the product attributes susceptible to change during storage and likely to influence quality, safety and/or efficacy demonstrated similar degradation profiles between representative batches of RTXM83 and the RMP (data not shown).

3.6 Biological Activities

We have previously shown that RTXM83 and RMP are similar in terms of human CD20 recognition and ADCC induction [18]. Now, we present extended characterization of the biological potency of our biosimilar by evaluating all three known rituximab mechanisms of action along with binding experiments to the C1q and a complete panel of FcRs.

The strength of the RTXM83:CD20 interaction has now been analysed in a cell-based ELISA assay using CD20+ human lymphoma cells. In agreement with our previous flow cytometry results, this study showed that both antibody products bind to membrane CD20 with similar affinity (Table 2). Rituximab-induced apoptosis was then evaluated by Annexin V binding to cell surface phosphatidylserine molecules in CD20+ lymphoma cells. The results showed that the biosimilar can induce apoptosis in a dose-response manner and with comparable potency to RMP (Suppl. Fig. 10 and Table 2).
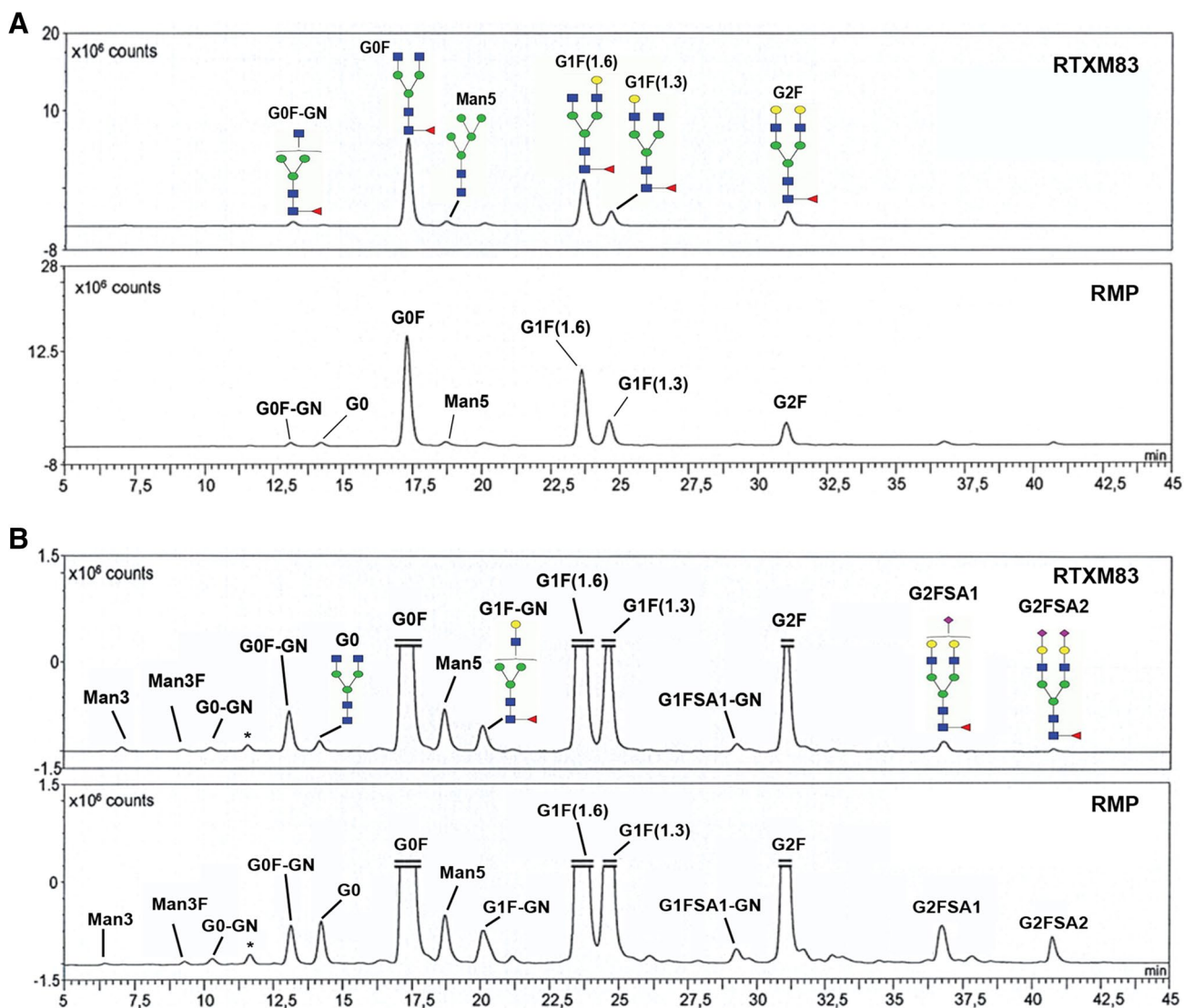
Fig. 5 N-glycosylation patterns of RTXM83 and RMP by NP-HPLC. **a** Representative elution profiles of 2-AB-labelled released *N*-glycans after NP-HPLC separation and fluorescence detection. **b** Magnification of the elution profiles to display low abundant peak signals. Glycan structures: Man3, $Man_3GlcNAc_2$; Man3F, $Man_3GlcNAc_2$ with α1,6-Fuc; G0-GN, diantennary w/o 2 β-Gal w/o 1 GlcNAc; G0F-GN, diantennary w/o 2 β-Gal w/o 1 GlcNAc with α1,6-Fuc; G0, diantennary w/o 2 β-Gal; G0F, diantennary w/o 2 β-Gal with α1,6-Fuc; Man5, $Man_5GlcNAc_2$; G1F-GN, diantennary w/o 1 β-Gal w/o 1 Glc-

NAc with α1,6-Fuc; G1F(1.6), diantennary w/o 1 β-Gal with α1,6-Fuc (Man6-isomer); G1F(1.3), diantennary w/o 1 β-Gal with α1,6-Fuc (Man3-isomer); G1FSA1-GN, monosialylated diantennary w/o 1 β-Gal w/o 1 GlcNAc with α1,6-Fuc; G2F, diantennary with α1,6-Fuc;G2FSA1, monosialylated diantennary with α1,6-Fuc; G2FSA2, disialylated diantennary with α1,6-Fuc. Non-carbohydrate contaminant peak signals are labelled by an asterisk. *2-AB* 2-aminobenzamide, *NP-HPLC* normal phase high-performance liquid chromatography, *RMP* reference medicinal product, *w/o* without

Similar to many other therapeutic monoclonal antibodies, rituximab mediates CDC and ADCC through the binding of its Fc region to C1q, and different Fcγ receptors expressed in the surface of various immune cells. ELISA experiments showed that RTXM83 and RMP bind to C1q with comparable potencies (Table 2). Furthermore, both rituximab products showed indistinguishable dose-response cytotoxicity curves and equivalent relative potency in CDC bioassays (Table 2 and Suppl. Fig. 10). The reporter gene-based ADCC

bioassay studies presented here confirmed that RTXM83 and RMP induced similar ADCC responses, displaying superimposable dose-dependent curves and reaching equivalent potency values (Table 2 and Suppl. Fig. 10).

Binding affinities to different Fcγ receptors and FcRn were then measured by SPR. The obtained K_D values were within the range described for these types of antibody:FcR interactions, including those reported for other rituximab:FcR interactions (Suppl. Table 5) [35–38].

Table 1 SEC and SV-AUC analysis of the RTXM83 biosimilar and reference product

Sample	MW (Da)	% species by SEC		% species by SV-AUC		
		Monomer	Dimer/HMW	Monomer	Dimer	HMW
RTXM83	149,441 ± 1007	99.5 ± 0.1	0.4 ± 0.1	96.2 ± 0.6	2.3 ± 0.7	1.0 ± 0.6
RMP	148,878 ± 169	99.1 ± 0.1	0.8 ± 0.1	96.1 ± 0.7	2.7 ± 0.4	1.2 ± 0.3

The reported values are mean ± SD. SEC samples consisted of ten batches of RMP and nine batches of RTXM83. SV-AUC samples consisted of four batches of RMP and three batches of RTXM83

HMW high molecular weight, *MW* molecular weight, *RMP* reference medicinal product, *SD* standard deviation, *SEC* size-exclusion chromatography, *SV-AUC* sedimentation velocity analytical ultracentrifugation

Statistical PLA analysis demonstrated that the relative binding responses of both rituximab products were equivalent (Table 2).

4 Discussion

Herein, we present the physicochemical and functional characterization of RTXM83, the first rituximab biosimilar developed and approved in South America. RTXM83 mass analysis revealed it has the expected molecular weight of rituximab and a primary sequence identical to the reference product. Disulfide bridges and amino acid modification patterns were non-distinguishable. Additionally, both products showed similarity in terms of the secondary, tertiary and quaternary structure conformation via a wide battery of analytical techniques (intrinsic fluorescence, CD, SLS, and micro-differential scanning calorimetry).

CEX and cIEF studies revealed that RTXM83 presents a slightly lower content of acidic species and a slightly higher content of basic species than RMP. Amino and carboxy-terminal integrity peptide mapping experiments showed that RTXM83 presents almost complete cyclization of its HC and LC N-terminal glutamines. Therefore, we attributed the slightly higher proportions of basic variants observed in RTXM83 to partial C-terminal lysine cleavage. This hypothesis was further confirmed by treatment of the products with carboxypeptidase B. C-terminal lysine removal is a type of PTM commonly found in native proteins [27, 39]; thus it should not be considered a regulatory concern. In fact, several antibody products with different extents of C-terminal lysine processing were shown to display equivalent biological potency in FcR-mediated functions and in pharmacokinetic and pharmacodynamic studies [40–43].

Quantitative NP-HPLC analysis revealed that the glycoform profile of RTXM83 was similar to that of the reference product, with slightly lower levels of total afucosylation and

Table 2 Summary of the biological in vitro potency and binding affinity for RTXM83 and the reference product

Function	RTXM83		RMP		Method
	Min–max	Mean ± 2 SD	Min–max	Mean ± 2 SD	
CD20 binding	91–121	103 ± 22.1	90–129	107 ± 22.3	Cell-based
Apoptosis	79–113	97 ± 24.8	74–126	101 ± 31.2	Cell-based
C1q binding	90–109	101 ± 13.2	101–110	106 ± 5.3	ELISA
CDC	83–101	94 ± 14.2	91–116	101 ± 18.2	Cell-based
ADCC	71–97	80 ± 18.0	76–109	89 ± 19.2	Cell-based
Fc-receptor binding					
FcRn	84–100	94 ± 12.1	91–106	100 ± 10.5	SPR
FcγRI	90–121	106 ± 19.2	100–125	108 ± 16.2	SPR
FcγRIIa	87–109	102 ± 14.1	100–122	109 ± 11.5	SPR
FcγRIIb	94–109	104 ± 10.1	100–121	110 ± 13.3	SPR
FcγRIIIa	89–111	97 ± 12.6	94–134	113 ± 23.9	SPR

The results are expressed as the relative potency (%) or binding affinity (%) of each sample compared against an RTXM83 in-house reference standard. Parallelism was determined using a 95% CI ($n = 9$ for RTXM83 and $n = 10$ for RMP)

ADCC antibody-dependent cell-mediated cytotoxicity, *CDC* complement-dependent cytotoxicity, *CI* confidence interval, *ELISA* enzyme-linked immunosorbent assay, *FcγR* Fcγ receptor, *FcRn* neonatal Fc receptor, *RMP* reference medicinal product, *SD* standard deviation, *SPR* surface plasmon resonance

galactosylation in the biosimilar. However, as demonstrated in all subsequent biological assays presented here, these differences had no impact in RTXM83's FcR binding affinity or ADCC and CDC potency. As anticipated in the biosimilar guidelines [44], such minor variability is contemplated for a biological manufacturing process. Indeed, MabThera®/Rituxan® batch analyses across the lifetime of the market product revealed drastic changes in both the charge variant distributions and *N*-glycan profiles [45]. Thus, the differences observed between RTXM83 and RMP batches can be considered comparable to and within the expected range of variation that can be observed for recombinant mAbs manufacture.

Sialylation is another critical PTM for therapeutic proteins. In particular, NGNA sialic acid constitutes a potential cause of immunogenicity when administered in therapeutic treatments, due to its absence or low abundance in human proteins [46, 47]. Quantitative analysis of NGNA and NANA demonstrated that both products have low and comparable amounts of each of these sialylated glycoforms, suggesting that no NGNA-related immunogenicity issues should be expected. Hence, it can be concluded that the RTXM83 biosimilar and reference product have comparable profiles in terms of PTMs, including biologically relevant charge and glycosylation variants.

Protein aggregation remains as an important concern of biological therapies because of the potential of induced immunogenicity, and thus a CQA to evaluate during the development and production of biologic products. SEC, SV-AUC, DLS, and CE-SDS studies demonstrated that RTXM83 and RMP have comparable contents of monomer, dimer and HMW aggregates, indicating that no differences in immunogenicity issues related to protein aggregation should be expected.

The clinical efficacy of rituximab is currently considered to be determined by the outcome of complex and dynamic interactions of three major mechanisms of target cell destruction—CDC, ADCC, and apoptosis induction through CD20 cross-linking signalling [48–50]—rendering it critical for any rituximab biosimilar to be approved to match all the described mechanisms of action of the reference product. Previous ADCC experiments demonstrated similarity between RTXM83 and the reference product in the classical colorimetric lactate dehydrogenase (LDH) cytotoxicity assay [18]. Furthermore, RTXM83 displayed the same potency as the reference product regarding the FcγRIIIa-158 F/V polymorphism variants of the effector cells, showing a greater ADCC response with effector cells bearing the V/V and V/F dimorphisms than to the F/F variant. In addition to these previous findings, all functional experiments presented here demonstrated that RTXM83 and RMP have similar potency in all described rituximab biological functions, suggesting

that it would induce the same antibody-mediated immune cytotoxic responses as the reference product in vivo.

The biosimilar manufacturing industry is flourishing in emerging markets such as Latin America and Asia, where biosimilar adoption represents a strategic avenue to provide high quality and clinically effective medications at a reduced cost. In Latin America, regulatory authorities have begun establishing well-defined and standardized pathways for biosimilar market registration, with countries such as Brazil and Argentina already counting with regulatory guidelines. The similarity between RTXM83 and the reference product MabThera®/Rituxan® with respect to efficacy, safety, and tolerability has been recently demonstrated at the clinical level in a prospective, phase III, multicentre clinical trial (NCT02268045) with diffuse large B-cell lymphoma patients [22]. This clinical trial, along with the physicochemical and biological studies presented here, led to RTXM83 approval as the first rituximab biosimilar in South America and its commercialization in several Latin American, Middle Eastern and African countries. Post-marketing surveillance studies in Argentina demonstrated that the safety profile of RTXM83 (Novex®) is similar to that of the reference product [51].

5 Conclusions

Here, we demonstrate that RTXM83 is a rituximab biosimilar developed under the rigorous guidelines of international regulatory agencies. The comparative analytical characterization between RTXM83 and its reference product demonstrated high similarity in all product CQAs, translating into equivalent biological potency and similar mechanisms of action. RTXM83 has been recently approved as the first rituximab biosimilar in South America and is marketed in several low income countries worldwide.

Compliance with Ethical Standards

References

1. Reff ME, Carner K, Chambers KS, Chinn PC, Leonard JE, Raab R, et al. Depletion of B cells in vivo by a chimeric mouse human monoclonal antibody to CD20. Blood. 1994;83(2):435–45.
2. Maloney DG, Grillo-Lopez AJ, White CA, Bodkin D, Schilder RJ, Neidhart JA, et al. IDEC-C2B8 (rituximab) anti-CD20

monoclonal antibody therapy in patients with relapsed low-grade non-Hodgkin's lymphoma. Blood. 1997;90(6):2188–95.

3. Maloney DG, Liles TM, Czerwinski DK, Waldichuk C, Rosenberg J, Grillo-Lopez A, et al. Phase I clinical trial using escalating single-dose infusion of chimeric anti-CD20 monoclonal antibody (IDEC-C2B8) in patients with recurrent B-cell lymphoma. Blood. 1994;84(8):2457–66.

4. Salles G, Barrett M, Foa R, Maurer J, O'Brien S, Valente N, et al. Rituximab in B-cell hematologic malignancies: a review of 20 years of clinical experience. Adv Ther. 2017;34(10):2232–73.

5. Gurcan HM, Keskin DB, Stern JN, Nitzberg MA, Shekhani H, Ahmed AR. A review of the current use of rituximab in autoimmune diseases. Int Immunopharmacol. 2009;9(1):10–25.

6. Sanz I. Indications of rituximab in autoimmune diseases. Drug Discov Today Ther Strateg. 2009;6(1):13–9.

7. European Medicines Agency. Guideline on similar biological medicinal products containing biotechnology-derived proteins as active substance: non-clinical and clinical issues. 2014. http://www.ema.europa.eu/docs/en_GB/document_library/Scientific_guideline/2015/01/WC500180219.pdf2014. Accessed 20 Sep 2018.

8. World Health Organization. Guidelines on evaluation of monoclonal antibodies as similar biotherapeutic products (SBPs). 2016. http://www.who.int/biologicals/expert_committee/mAb_SBP_GL-ECBS_review_adoption-2016.10.26-11.7post_ECBS-Clean_Version.pdf. Expert Committee on Biological Standardization. Accessed 18 Sep 2018.

9. US Food and Drug Administration. Guidance for industry: quality considerations in demonstrating biosimilarity of a therapeutic protein product to a reference product. 2015. http://www.fda.gov/downloads/drugs/guidancecomplianceregulatoryinformation/guidances/ucm291134.pdf2015. Accessed 18 Sep 2018.

10. ANMAT. Disposición No. 7729/11. 2011. http://www.anmat.gov.ar/boletin_anmat/noviembre_2011/Dispo_7729-11.pdf2011. Accessed 10 Dec 2018.

11. Garcia R, Araujo DV. The regulation of biosimilars in Latin America. Curr Rheumatol Rep. 2016;18(3):16.

12. Ministry of Public Health of Uruguay. Decreto No. 38/015. Documento de Registro de Medicamentos Biotecnológicos. 2015. Accessed 18 Dec 2018.

13. GaBI Online. Similar biotherapeutic products approved and marketed in Latin America. 2013. http://www.gabionline.net/Biosimilars/General/Similar-biotherapeutic-products-approved-and-marketed-in-Latin-America. Accessed 14 Sep 2018.

14. National Institute of Public Health of Mexico. Norma Oficial Mexicana NOM-257-SSA1-2014, En materia de medicamentos biotecnológicos. 2014. http://dof.gob.mx/nota_to_doc.php?codnota=53755172014. Accessed 18 Dec 2018.

15. Anvisa. Resolução da Diretoria Colegiada_RDC No. 55. 2010. http://portal.anvisa.gov.br/documents/10181/2718376/RDC_55_2010_COMP.pdf/bb86b1c8-d410-4a51-a9df-a61e165b9618; Accessed 18 Dec 2018.

16. Butler M. Animal cell cultures: recent achievements and perspectives in the production of biopharmaceuticals. Appl Microbiol Biotechnol. 2005;68(3):283–91.

17. Hossler P, Khattak SF, Li ZJ. Optimal and consistent protein glycosylation in mammalian cell culture. Glycobiology. 2009;19(9):936–49.

18. Cuello HA, Segatori VI, Alberto M, Pesce A, Alonso DF, Gabri MR. Comparability of antibody-mediated cell killing activity between a proposed biosimilar RTXM83 and the originator rituximab. BioDrugs Clin Immunother Biopharm Gene Ther. 2016;30(3):225–31.

19. Cartron G, Dacheux L, Salles G, Solal-Celigny P, Bardos P, Colombat P, et al. Therapeutic activity of humanized anti-CD20 monoclonal antibody and polymorphism in IgG Fc receptor FcgammaRIIIa gene. Blood. 2002;99(3):754–8.

20. Hatjiharissi E, Xu L, Santos DD, Hunter ZR, Ciccarelli BT, Verselis S, et al. Increased natural killer cell expression of CD16, augmented binding and ADCC activity to rituximab among individuals expressing the Fc{gamma}RIIIa-158 V/V and V/F polymorphism. Blood. 2007;110(7):2561–4.

21. Treon SP, Hansen M, Branagan AR, Verselis S, Emmanouilides C, Kimby E, et al. Polymorphisms in FcgammaRIIIA (CD16) receptor expression are associated with clinical response to rituximab in Waldenstrom's macroglobulinemia. J Clin Oncol. 2005;23(3):474–81.

22. Candelaria M, Gonzalez D, Fernandez Gomez FJ, Paravisini A, Del Campo Garcia A, Perez L, et al. Comparative assessment of pharmacokinetics, and pharmacodynamics between RTXM83, a rituximab biosimilar, and rituximab in diffuse large B-cell lymphoma patients: a population PK model approach. Cancer Chemother Pharmacol. 2018;81(3):515–27.

23. Idusogie EE, Presta LG, Gazzano-Santoro H, Totpal K, Wong PY, Ultsch M, et al. Mapping of the C1q binding site on rituxan, a chimeric antibody with a human IgG1 Fc. J Immunol. 2000;164(8):4178–84.

24. Lefranc M-P. IMGT®, the international ImMunoGeneTics information system®. Montpellier, France. http://www.imgt.org. Accessed 26 Mar 2019.

25. Beck A, Diemer H, Ayoub D, Debaene F, Wagner-Rousset E, Carapito C, et al. Analytical characterization of biosimilar antibodies and Fc-fusion proteins. TrAC Trends Anal Chem. 2013;48:81–95.

26. Du Y, Walsh A, Ehrick R, Xu W, May K, Liu H. Chromatographic analysis of the acidic and basic species of recombinant monoclonal antibodies. mAbs. 2012;4(5):578–85.

27. Liu H, Gaza-Bulseco G, Faldu D, Chumsae C, Sun J. Heterogeneity of monoclonal antibodies. J Pharm Sci. 2008;97(7):2426–47.

28. Walsh G, Jefferis R. Post-translational modifications in the context of therapeutic proteins. Nat Biotechnol. 2006;24(10):1241–52.

29. Sinha S, Pipes G, Topp EM, Bondarenko PV, Treuheit MJ, Gadgil HS. Comparison of LC and LC/MS methods for quantifying N-glycosylation in recombinant IgGs. J Am Soc Mass Spectrom. 2008;19(11):1643–54.

30. Rustandi RR, Washabaugh MW, Wang Y. Applications of CE SDS gel in development of biopharmaceutical antibody-based products. Electrophoresis. 2008;29(17):3612–20.

31. Clodfelter DK, Nussbaum MA, Reilly J. Comparison of free solution capillary electrophoresis and size exclusion chromatography for quantitating non-covalent aggregation of an acylated peptide. J Pharm Biomed Anal. 1999;19(5):763–75.

32. den Engelsman J, Garidel P, Smulders R, Koll H, Smith B, Bassarab S, et al. Strategies for the assessment of protein aggregates in pharmaceutical biotech product development. Pharm Res. 2011;28(4):920–33.

33. Gabrielson JP, Brader ML, Pekar AH, Mathis KB, Winter G, Carpenter JF, et al. Quantitation of aggregate levels in a recombinant humanized monoclonal antibody formulation by size-exclusion chromatography, asymmetrical flow field flow fractionation, and sedimentation velocity. J Pharm Sci. 2007;96(2):268–79.

34. Grinberg N, Blanco R, Yarmush DM, Karger BL. Protein aggregation in high-performance liquid chromatography: hydrophobic interaction chromatography of beta-lactoglobulin A. Anal Chem. 1989;61(6):514–20.

35. Montacir O, Montacir H, Eravci M, Springer A, Hinderlich S, Saadati A, et al. Comparability study of rituximab originator and follow-on biopharmaceutical. J Pharm Biomed Anal. 2017;5(140):239–51.

36. Nupur N, Chhabra N, Dash R, Rathore AS. Assessment of structural and functional similarity of biosimilar products: rituximab as a case study. mAbs. 2018;10(1):143–58.

37. Saxena A, Wu D. Advances in therapeutic Fc engineering—modulation of IgG-associated effector functions and serum half-life. Front Immunol. 2016;7:580.

38. Visser J, Feuerstein I, Stangler T, Schmiederer T, Fritsch C, Schiestl M. Physicochemical and functional comparability between the proposed biosimilar rituximab GP2013 and originator rituximab. BioDrugs Clin Immunother Biopharm Gene Ther. 2013;27(5):495–507.

39. Harris RJ. Processing of C-terminal lysine and arginine residues of proteins isolated from mammalian cell culture. J Chromatogr A. 1995;705(1):129–34.

40. Antes B, Amon S, Rizzi A, Wiederkum S, Kainer M, Szolar O, et al. Analysis of lysine clipping of a humanized Lewis-Y specific IgG antibody and its relation to Fc-mediated effector function. J Chromatogr B Anal Technol Biomed Life Sci. 2007;852(1–2):250–6.

41. Dick LW Jr, Qiu D, Mahon D, Adamo M, Cheng KC. C-terminal lysine variants in fully human monoclonal antibodies: investigation of test methods and possible causes. Biotechnol Bioeng. 2008;100(6):1132–43.

42. Hong J, Lee Y, Lee C, Eo S, Kim S, Lee N, et al. Physicochemical and biological characterization of SB2, a biosimilar of Remicade (R) (infliximab). mAbs. 2017;9(2):364–82.

43. Khawli LA, Goswami S, Hutchinson R, Kwong ZW, Yang J, Wang X, et al. Charge variants in IgG1: isolation, characterization, in vitro binding properties and pharmacokinetics in rats. mAbs. 2010;2(6):613–24.

44. European Medicines Agency. Guideline on similar biological medicinal products containing monoclonal antibodies—non-clinical and clinical issues. 2012. https://www.ema.europa.eu/documents/scientific-guideline/guideline-similar-biological-medicinal-products-containing-monoclonal-antibodies-non-clinical_en.pdf. Accessed 10 Jan 2019.

45. Schiestl M, Stangler T, Torella C, Cepeljnik T, Toll H, Grau R. Acceptable changes in quality attributes of glycosylated biopharmaceuticals. Nat Biotechnol. 2011;29(4):310–2.

46. Ghaderi D, Taylor RE, Padler-Karavani V, Diaz S, Varki A. Implications of the presence of N-glycolylneuraminic acid in recombinant therapeutic glycoproteins. Nat Biotechnol. 2010;28(8):863–7.

47. Varki A. Loss of N-glycolylneuraminic acid in humans: mechanisms, consequences, and implications for hominid evolution. Am J Phys Anthropol. 2001;33:54–69.

48. Cerny T, Borisch B, Introna M, Johnson P, Rose AL. Mechanism of action of rituximab. Anticancer Drugs. 2002;13(Suppl 2):S3–10.

49. Smith MR. Rituximab (monoclonal anti-CD20 antibody): mechanisms of action and resistance. Oncogene. 2003;22(47):7359–68.

50. Weiner GJ. Rituximab: mechanism of action. Semin Hematol. 2010;47(2):115–23.

51. Milone G, Penna M, Fernández F, Spitzer E, Millan S, De Caso P, et al. Post-marketing surveillance with a biosimilar of rituximab (Novex®) in Argentina. 59th ASH annual meeting; Atlanta; 2017. p. 2131.